COLLIDING BEAMS EXPERIMENT

Burton Richter,
University of Stanford.

Let me begin by saying that we all hope that this will be the last talk about what we are going to do when the experiment is ready. We hope that next year we can talk about what we have done. The physicists associated with the project are B. Gittelman and G.K. O'Neill, at Princeton, and W.C. Barber, W.K.H. Panofsky, and myself, at Stanford. Most of the work that has been done on the project has been done by J. Walling (mechanical design and engineering), L. Bogart (magnetic measurements and field corrections), N. Dean (vacuum system), G. Gleason (electronics), and C. Noyer (rf).

Since most people are familiar with the general plan of the experiment, I shall review it only briefly. We will use the Stanford electron linear accelerator as a source of electrons to fill two storage rings with one common straight section to a circulating current of 1 amp in each ring ($\sim 3 \cdot 10^{11}$ in a bunch). The energy of each beam at injection will be about 500 MeV. The two beams will collide in the common straight section, and the elastically scattered electrons which come off back-to-back in their centre-of-mass system will be counted in coincidence by an array of counters which surround the interaction region. Figure 1 shows a top view of the experimental arrangement.

The unanalysed beam from the linear accelerator is piped in vacuum a distance of 40 metres from the end of the accelerator to the storage ring area. The first steering magnet shown in the figure is off. The beam is carried through the other two dc steering magnets into a slot cut in the side yoke of one of the storage ring quadrants, and is brought to the gap of the pulsed inflector. In this quadrant the beam leaves the 10^{-6} mm vacuum of the transport system and enters the 10^{-9} mm vacuum of the storage rings. At the pulsed inflector the beam is about 6 cm from the equilibrium orbit and makes an angle of about 0.03 radian with respect to the equilibrium orbit. The pulsed inflector changes this angle to zero. This pulsed magnet is turned off after a time corresponding to two turns around the ring. Two

turns later, betatron oscillations bring the first bunch injected back to the gap of the pulsed magnet, but the field is zero by then. Figure 2 shows a phase diagram of the beam at the inflector position for the first few turns. The radiation damping of the betatron and synchrotron oscillations makes the injected electrons form a flat ribbon of charge travelling on the equilibrium orbit whose radial position is determined by the rf cavity frequency. Since the radiation damping times are around 10 msec and the time between accelerator pulses is around 16 msec, the pulsed magnet can be turned on at the time of the next accelerator burst without affecting the beam already captured. Injection into the first ring will continue until the desired circulating beam is built up. The first steering magnet is then turned on and the other ring is filled in the same fashion.

If all our calculations are correct, the lifetime of the stored beam should be about 15-20 hours. The two smallest limits on the lifetime are given by the processes of bremsstrahlung in the residual gas and electron-electron scattering from the gas atoms. All other processes that we have considered give lifetime limits at least a factor of 10 larger than this.

In the first experiment we plan to cover a range of 4-momentum transfers in the direct diagram of from 100 to 700 MeV/c. To cover the range we must change the energy of the electrons in the ring. This will be done by reducing the field in the storage rings after the rings have been filled. The synchrotron radiation will make the beam energy track the field.

I thought I would next describe the status of the various components. The simplest in conception and one involving the most standard construction practices is, of course, the magnet. Figure 3 shows a cross-section through one of the quadrants. As you can see, the magnets are fairly small. The gap is 6.3 cm high by 25 cm wide. The central orbit radius is 140 cm, and the field corresponding to 500 MeV electrons circulating at this radius is 12,000 gauss. The straight sections between magnets are about 70 cm long. The total weight of iron and copper in two rings is 46 tons. The power required to drive them to 12,000 gauss is 420 kilowatts. Figure 4 shows the finished shells of the Y-magnets that are at each end of the interaction region. Figure 5 shows one of the

quadrants during construction, before the pole-end contour had been cut. Figure 6 shows the experimental area with all magnets in place. Figure 7 shows a plot of the magnetic field gradient in one of the n = 1 regions at several different fields. The gradient must be good all the way across the vacuum chamber only at the injection field. At other fields, only about ± 1 inch of good field is required.

The rf system is complete. It was designed to provide 10 kilowatts of rf power at cavity voltages up to 20 kW. At our design current of 1 amp in each ring, the power required to be delivered to the two beams to maintain them at 500 MeV is 8 kW. Losses in the cavities come to about 2 kW. The rf system has been tested at full power at full voltage and appears to function properly.

Figure 8 is a photograph of one of the pulsed inflector magnets. It operates as a lumped constant delay line, the ferrite yoke making the inductance with capacitors distributed uniformly along the main current lead. The line will be terminated in its characteristic impedance, about 11 ohms. Two of these units make up one pulsed inflector. The two sub-assemblies are driven in parallel by a line pulser with an output impedance of 5.5 ohms. These units have been pulsed in vacuum at full voltage (50 kV) and worked satisfactorily. The rise time of the pulse is 20 mμsec, and the delay time through the magnet is 90 mμsec. The magnetic field in the inflector gap has been measured and found to be constant over the pulse to better than 10%.

The vacuum chamber is finished. Each separate piece has been baked and pumped to a vacuum of $3 \cdot 10^{-10}$ mm. The complete vacuum chamber has been assembled and tested at Princeton, where it reached a pressure of 10^{-8} mm after one hour of baking. It has been disassembled and shipped to Stanford.

Figure 9 shows a side view of the interaction region. Note that the beams do not collide head-on. The vertical steering magnets indicated on the figure distort the equilibrium orbit so that the beams cross only in a small region at the centre of the straight section. The counters will be distributed over the sphere with the smallest counter angle being 40° rather than 35° as shown in the figure, and the counters will be close to the dome to minimize the multiple scattering loss. Table I shows some of the

parameters of the counting system (6 counter pairs at 40° and 16 at 90°). The cross-sections are computed for 500 MeV beams, and the counting rates for 1 amp in each ring.

Table I

Minimum angle	40°	
Number of counters	96	maximum
$d\sigma/d\Omega$ (40°)	$1.6 \cdot 10^{-30}$	cm^2
$\Delta\Omega$ (40°)	0.17	steradian
Count rate (40°)	0.80	counts/sec
$d\sigma/d\Omega$ (90°)	$0.18 \cdot 10^{-30}$	cm^2
$\Delta\Omega$ (90°)	0.44	steradian
Count rate (90°)	0.85	counts/sec

Figure 10 shows a drawing of what a counter assembly will look like. The counter itself is a ½" thick plastic scintillator, 2" in diameter. The light pipe is a glass tube aluminized on the inside. The magnetic shield has been tested in a field of 300 gauss. It consists of an outer shield of ⅛" thick low-carbon steel and an inner shield of 0.050" mumetal. All the parts for the counters, except the scintillators, have been delivered or will arrive within the next four weeks.

The counting electronics consist of a tunnel-diode discriminator and a tunnel-diode coincidence circuit. These are now being mass-produced and will be finished within the next six weeks.

Recently we have been studying the injection orbits into the storage rings using the linear accelerator electron beam as a probe. One must try to match the phase space acceptance of the storage ring to the accelerator beam. As the beam enters the storage ring and travels over the magnet coils, it finds itself in regions of very strong field gradient. We can reduce some of this by placing iron shims in the coil region to contour the field properly. These shims cannot, however, be continued on to the magnet pole without seriously affecting the focusing properties of the main field. Hence, a fairly large region of strong gradient is left. We have tried to compensate for this by adjusting the focusing properties of the

steering magnets which bring the beam to the storage rings. We seem to have been very lucky. The accelerator beam is about 1 cm in diameter at the entrance to the first steering magnet and has an angular divergence of about 10^{-4} radian. At the position of the pulsed inflector the beam is about $\frac{1}{2}$ cm high with an angular divergence of less than 0.002 radian. The dispersion of the injecting system spreads the beam out radially and loses us 80% of the incident electron beam. This loss is due to the radial acceptance of the pulsed magnet. Our measurements show that unless something is wrong with the storage ring field, our capture efficiency should be between 5% and 10% of the electrons which enter the ring in the useful two-turn injection period, which means about $2 \cdot 10^{8}$ electrons captured per accelerator pulse. From these measurements we estimate that the filling time for each ring will be about one minute.

Our future time schedule has one major uncertainty in it. The vacuum chamber is now being assembled at Stanford. We estimate that it should be ready to be installed in the storage rings in two to three months. We then have to store a beam. If you are a great optimist, you might believe that one minute after we turn the rings on, we will have a circulating current of one ampere. We are not quite such optimists, and I think that no-one associated with the turn-on of any synchrotron would be, either. If all goes well, we should be counting scattered particles in four or five months.

Our plans are for an experiment with an over-all error at each point on the angular distribution of about 3%. If we use as our criterion for finding an effect that our results must differ from the predictions of electrodynamics by three times the error, then we should be able to measure a cut-off in the photon propagator, for example, at $3 \cdot 10^{3}$ MeV/c. In terms of some modification at the electron vertex, we should be able to see an effect at an electron mean square radius of about $1 \cdot 10^{-14}$ cm.

Positron Experiments

Whenever this subject has been brought up in the past, we have refused to commit ourselves about its prospects. I am not going to change this policy, but I would like to discuss the difficulties of the positron experiments a bit.

First there are some technical problems. The electrons and positrons must be made to circulate in opposite senses in the same magnet. The beams still must be prevented from colliding head on for the same reasons as in the electron-electron scattering experiment. The rf cavity and the interaction region must be shifted so that they are opposite each other. A new steering and inflecting system must be constructed. A new counting system will be needed. We can solve all these problems in time. However, the positron experiments are incompatible with the e^--e^- scattering experiments and so we must finish e^--e^- before starting e^+-e^-.

These problems are not the main reason for our long-standing silence on the experiment. The electron scattering experiments must work fairly well for the positron experiments to work at all. Table II shows the cross-sections in the centre-of-mass system for several processes of interest considering only first order electromagnetic interactions. Figure 11 shows

Table II

$e^- + e^- \rightarrow e^- + e^-$	$\frac{d\sigma}{d\Omega} = \frac{\alpha^2}{8\,E^2}\left[\frac{1+\cos^4(\Theta/2)}{\sin^4(\Theta/2)} + \frac{1+\sin^4(\Theta/2)}{\cos^4(\Theta/2)} + \frac{2}{\sin^2(\Theta/2)\cos^2(\Theta/2)}\right]$
$e^+ + e^- \rightarrow e^+ + e^-$	$\frac{d\sigma}{d\Omega} = \frac{\alpha^2}{8\,E^2}\left[\frac{1+\cos^4(\Theta/2)}{\sin^4(\Theta/2)} - \frac{\cos^2(\Theta/2)}{\sin^2(\Theta/2)} + 2\cos^4(\Theta/2)\right]$
$e^+ + e^- \rightarrow \mu^+ + \mu^-$	$\frac{d\sigma}{d\Omega} = \frac{\alpha^2\beta}{16E^2}(2 - \beta^2\sin^2\Theta)$
$e^+ + e^- \rightarrow \pi^+ + \pi^-$	$\frac{d\sigma}{d\Omega} = \frac{\alpha^2\beta^3}{32E^2}\sin^2\Theta$

these cross-sections plotted as angle for a total centre-of-mass energy of 1000 MeV. The cross-sections for μ^+-μ^- and π^+-π^- production are very much smaller than for electron-electron or positron scattering. It is not quite as bad as it looks because the greatest interest in those processes proceeding through the e^+-e^- annihilation diagram is in the total cross-section.

The positron beam which we now have at Stanford has an intensity of about 10^{-4} of the electron beam. We may be able to improve it a little,

but probably not by as much as a factor of 10 without rebuilding the injection end of the accelerator. With this small beam we need a good capture efficiency, a fairly long beam life, and a small stored beam size to do any experiment at all. On the other hand, the electron-electron scattering experiment is quite a bit overdesigned. If we achieve a circulating beam intensity of 100 ma and a lifetime of greater than 2 minutes, we can do a very good experiment. Until we know what we can do in storing a beam, we cannot say anything about the positron experiment.

* * *

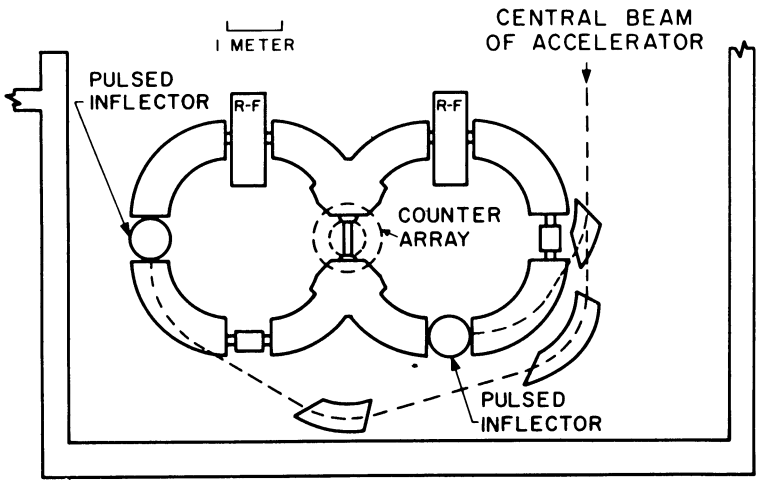

Fig. 1. Top view of experimental arrangement.

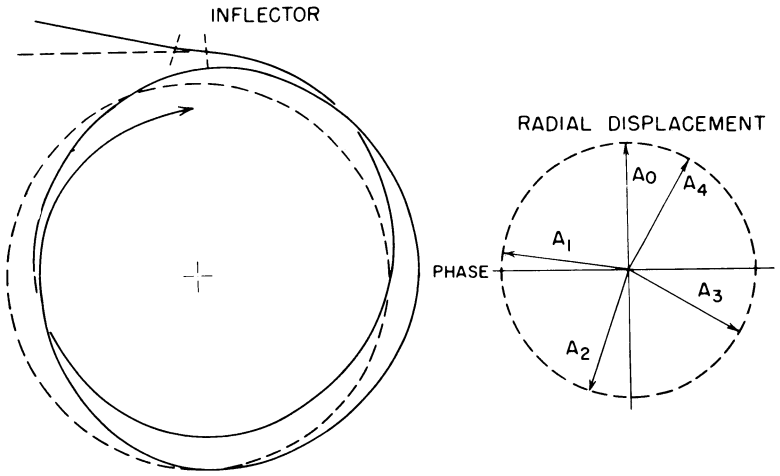

Fig. 2. Phase diagrams of beam at inflector for first few turns.

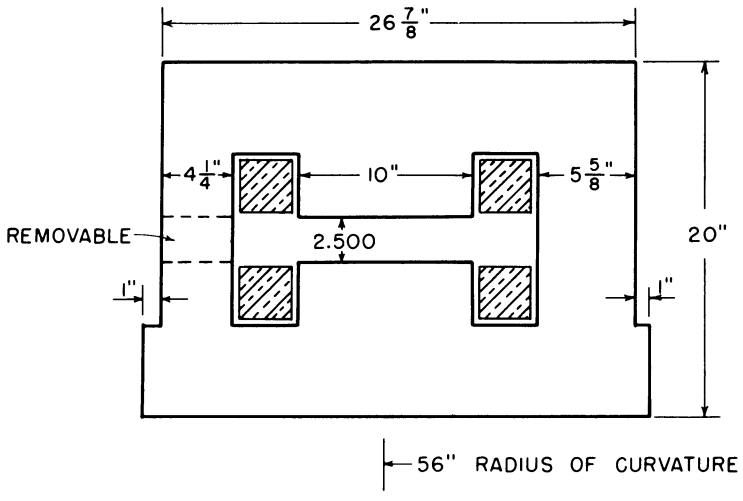

Fig. 3. Cross-section of magnet quadrant.

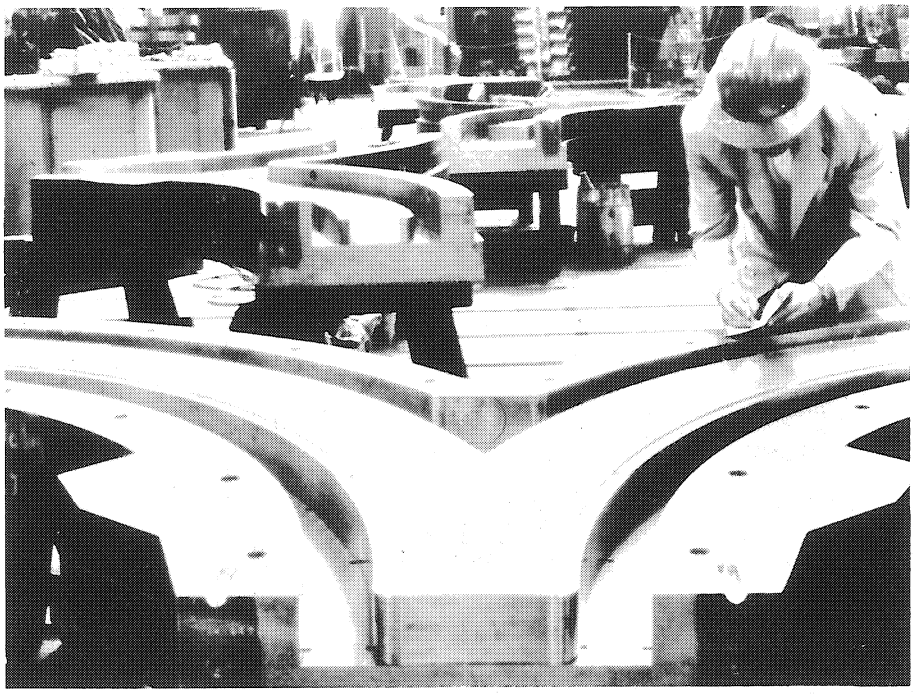

Fig. 4. Finished shells of Y-magnets at each end of interaction region.

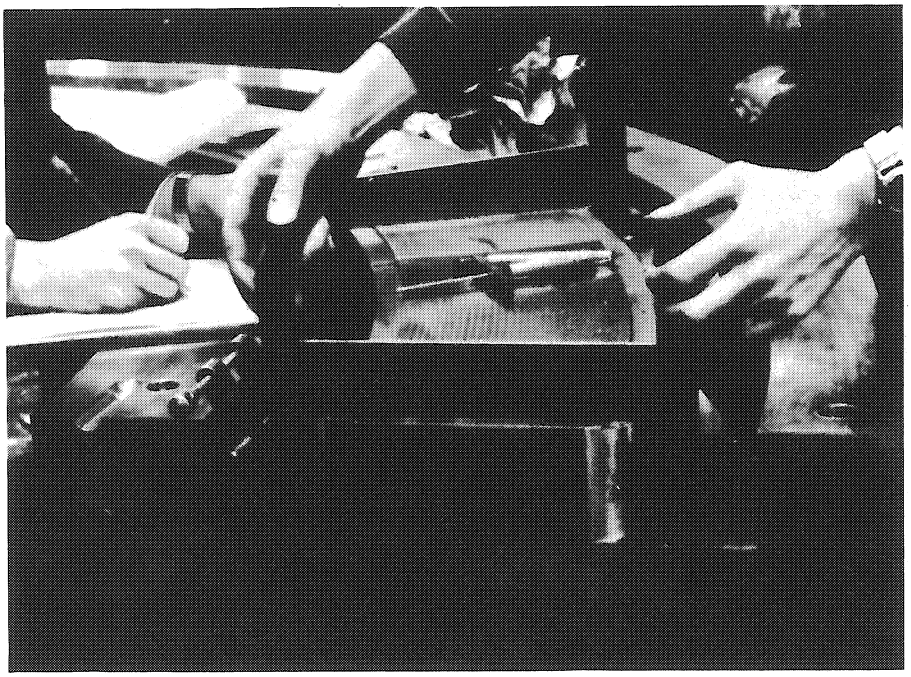

Fig. 5. One of the quadrants during construction.

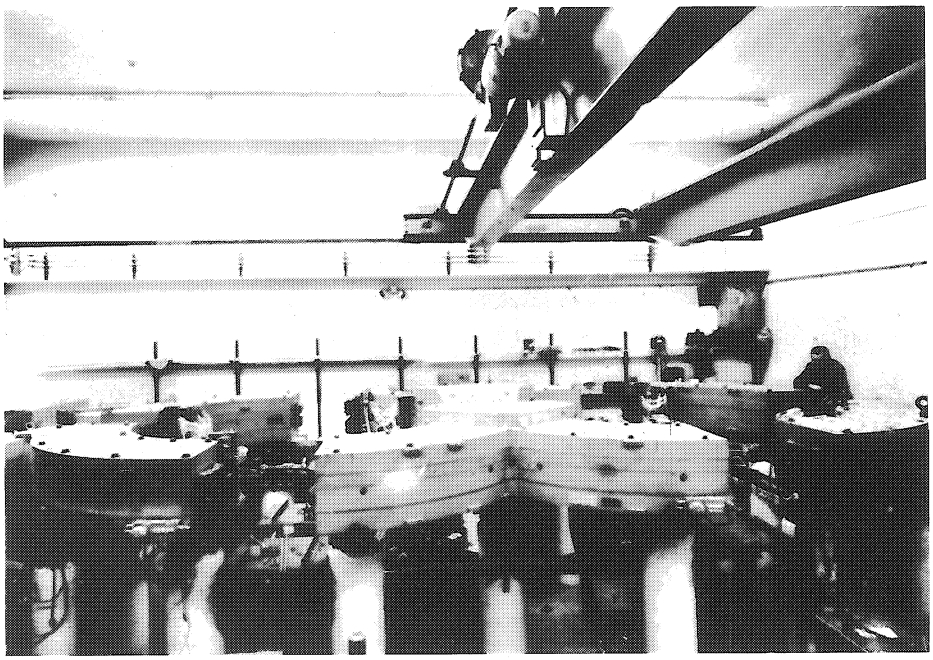

Fig. 6. Experimental area with all magnets in place.

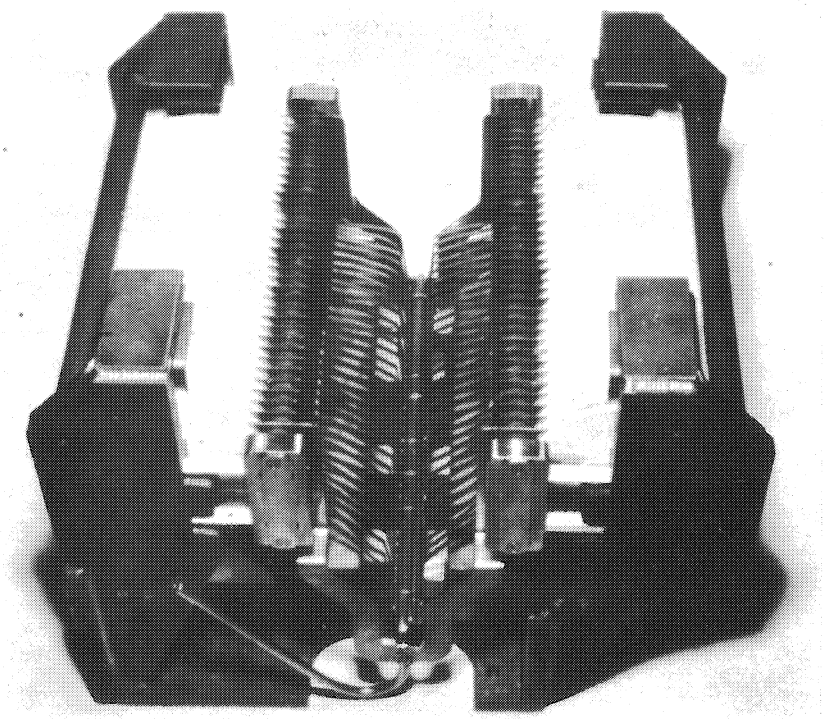

Fig. 8. One of the pulsed inflector magnets.

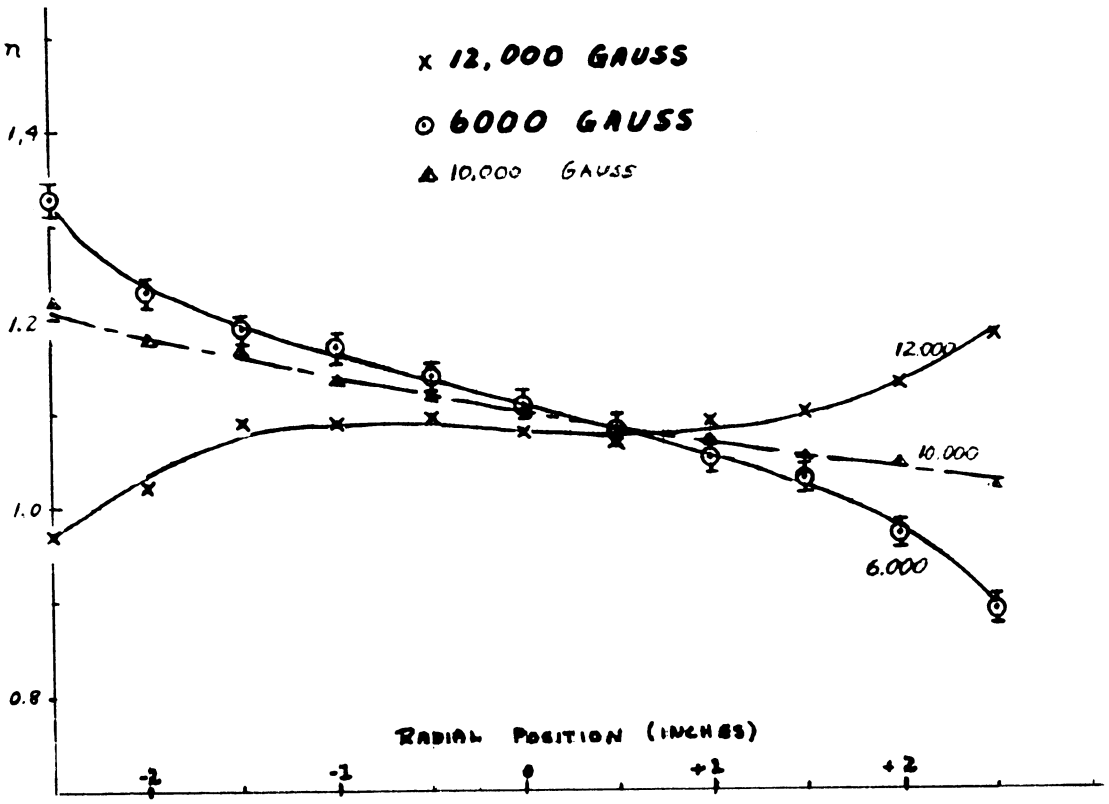

Fig. 7. Magnetic field gradient in one of the n = 1 regions at several different fields.

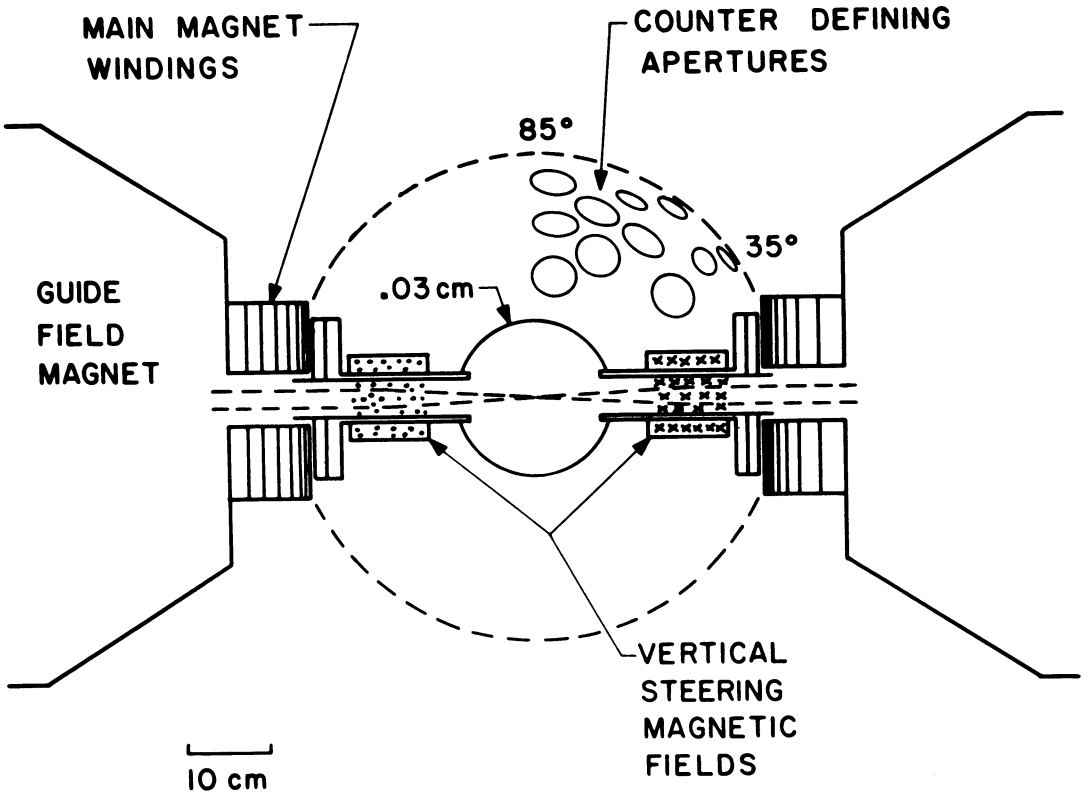

Fig. 9. Side view of interaction region.

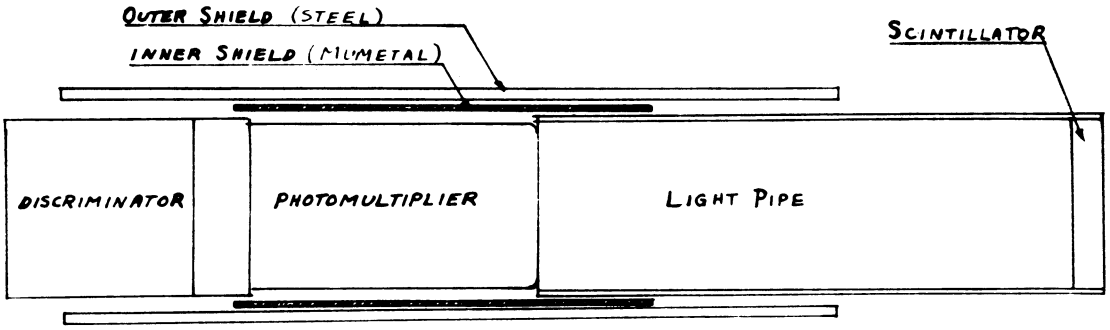

Fig. 10. Counter assembly.

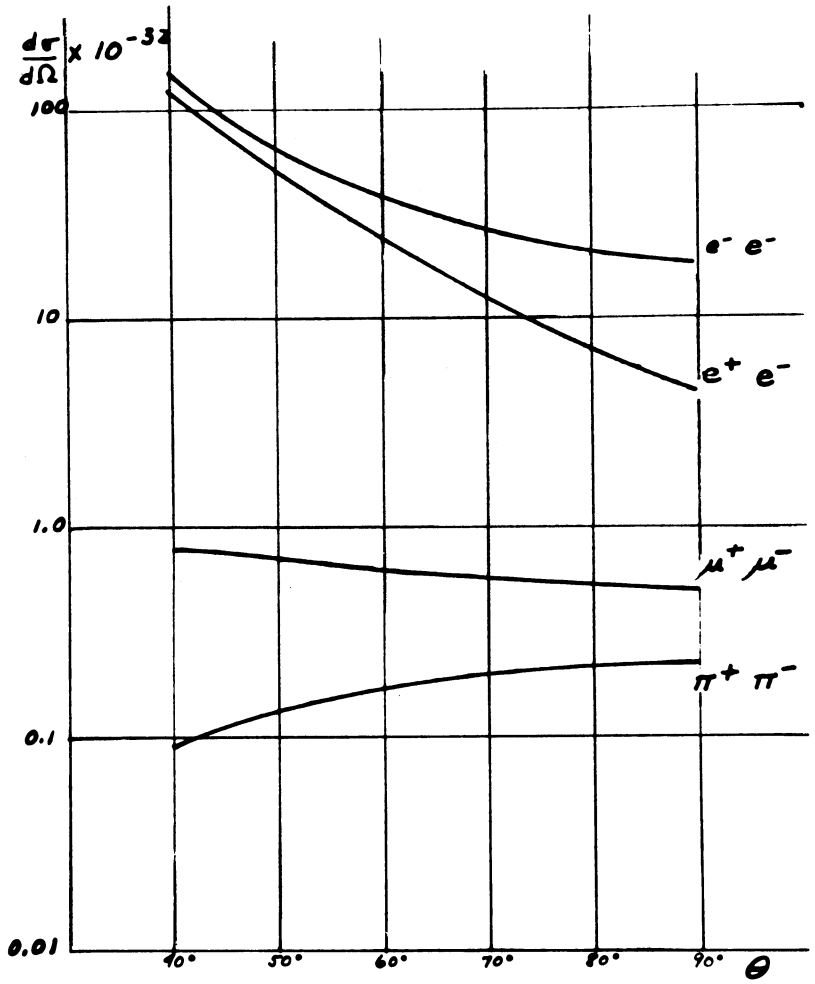

Fig. 11. Cross-sections for 1000 MeV c.m. energy.